Properties of pure and compound clusters of Si, Ge, and Pb

A. M. Mazzone
Consiglio Nazionale delle Richerche, Istituto Lamel, Via Gobetti 101, 40129 Bologna, Italy
(Received 11 August 1995; revised manuscript received 8 February 1996)

The properties of monoelemental Si, Ge, and Pb clusters and those of compound Si-Pb and Ge-Pb clusters have been studied by using semiempirical methods of the modified neglect of differential overlap type. The cluster size is $10 \leqslant N \leqslant 90$ and in compound clusters a fraction $\leqslant 0.5$ of Si and Ge atoms is replaced by Pb. The calculations support and extend the results of recent first-principles calculations of silicon clusters. They indicate, in fact, that for Si, Ge, and Pb elongated and spherical structures are both possible, the first lying lower in binding energy at large N. Noticeable relaxation is observed in compound clusters whose binding energies, bond lengths, and angles are substantially altered, with respect to the monoelemental ones, by the inclusion of the metallic element. [S0163-1829(96)06531-9]

I. INTRODUCTION

Recently, many experimental and theoretical studies have been concentrated on metal-semiconductor interfaces of the Pb-Ge and Pb-Si type. In fact, these structures are considered model candidates for the study of two-dimensional phenomena as Pb is insoluble in both bulk Ge and Si and does not alloy, intermix, or form strong chemical bonds over a wide temperature range. However, the Pb surface phases have turned out to be quite rich and the debate over their structure has continued for more than a decade. Furthermore, many controversies[1] are at present centered on experimental electron energy-loss spectroscopy (EELS) observations[2] which indicate that, contrary to the current concept that Pb represents a prototype metal overlayer, the interfaces of those structures are not abrupt and strong intermixing takes place.

This has obviously opened many problems about the diffusive motions of the deposited atoms and the bonding mode of these mixed structures. *Ab initio* molecular dynamics studies of film deposition[3,4] indicate a strong correlation of Pb with Ge, which, however, depends on the temperature of the deposition and on the surface coverage.

In this study we analyze the bonding mode of mixed metal-semiconductor structures and the problem is treated at the cluster level. The study of atomic clusters has become one of the most exciting areas of research as it offers the possibility of studying the transition from molecules to crystalline solids. This argument is particularly important for Si and Ge as in these materials cluster features are ubiquitous and appear inextricably connected with those of crystalline solids. The metallic behavior of liquid Ge, for instance, has been attributed to the interaction of the clusters formed in the melt. In Si the nonreactivity of large clusters has been explained on the basis of the similarity of the atomic arrangement with that of reconstructed Si surfaces.

Many calculations, *ab initio* and semiclassical, have been developed for Si clusters up to a size $N \sim 50$. On the contrary, since early work,[5] little attention has been paid to Ge and Pb though in recent years, spurred by the need for identifying unusual optical and thermal properties, there is a revival of interest in large clusters of these materials. Also, clusters with a composite structure, especially the ones combining metallic and covalent elements, are relatively unexplored, though it has been recently discussed that new kinds of materials could be obtained from the most stable of these clusters.[6] In this study we analyze the properties of monoelemental clusters of Si, Ge, and Pb and of compound clusters of the type Si/Pb and Ge/Pb. The cluster size is between medium and large and the calculation consists of an energy minimization using semiempirical methods of the modified neglect differential overlap (MNDO) type. At the expense of accurate details we have sought to elicit a few main models associated with the bonding between metallic and covalent atoms.

II. THE SIMULATION METHODS

For our calculations semiempirical methods of the molecular orbital (MO) type have been used. It is known that semiempirical methods rely on an extensive parametrization of the overlap exchange integrals and for this reason their validity may be uncertain for a charge configuration significantly different from the reference one. However, it is generally accepted that, if properly used, MO theory is a very powerful tool and provides a wealth of information, such as population analysis, wave functions, density, vibrational spectrum, ionization potential, hybridization, etc.

For this reason our study, in addition to the properties of clusters, presents a comparison of several semiempirical Hamiltonians. This has been intended as an overview of the limits of semiempirical calculations and has been made feasible through the use of the computer code MOPAC 6.0 developed by Stewart.[7] In MOPAC stable geometries are predicted by minimizing the total cluster energy, electronic and nuclear, with respect to atomic positions through standard and *ad hoc* gradient minimization techniques. The semiempirical Hamiltonians contained in MOPAC are modified in termediate neglect of differential overlap (MINDO), MNDO, PM3, and AM1. They differ in the level of approximation and parametrization. Furthermore, MINDO requires diatomic parameters while the others use only monatomic parameters. As the former are not available for the elements forming our clusters, MINDO was discarded and we use only

MNDO, PM3, and AM1. PM3 and AM1 use essentially the same approximations as MNDO except for a more sophisticated core-core repulsion term. However, a parametrization suitable for Pb is not available in AM1. Furthermore, a few test calculations have demonstrated that PM3 in Si and Ge leads to values of the binding energy and the ionization potential unrealistically large with respect to those of the crystal (that is, $E_b \sim 6$ eV for Si and $I_p \sim 10$ eV for Ge). In addition, for Ge, the convergence was found to be extremely slow. For these reasons MNDO and AM1 were used for Si and Ge and MNDO and PM3 for Pb. For a consistent comparison only MNDO was used in compound clusters.

A further option offered by MOPAC is that the dynamic evolution of the atom paths subject to nuclear and electronic forces and, possibly, to an initial impulse of kinetic energy can be calculated. These calculations [indicated in the following as dynamic reaction coordinate (DRC) paths] were used to test, in the ambiguous cases, the evolution and stability of the clusters. In those cases the DRC paths were compared with lattice thermal oscillations obtained from standard molecular dynamics calculations in crystalline silicon.[8] For the latter calculations a Tersoff potential in the form of Ref. 9 was adopted.

The results are compared with other theories and experiments, when available.

III. RESULTS

We presently examine clusters of size between medium and large ($10 \leqslant N \leqslant 90$). It is generally accepted that for this size the search for the lowest-energy structure is necessarily limited to a subset of the possible configurations and must be guided by physical insight or by developed models. For Si clusters an extensive theoretical investigation has shown that for $N \leqslant 10$ the stable structures with minimum energy have a compact form resulting from interlocked tetrahedra.[10–15] For $N \geqslant 20$ either elongated structures, formed by rings of five or six atoms, or spherical structures, formed by a core of tetrahedrally bonded atoms embedded in a cage whose mantel contains hexagonal and pentagonal rings, have been reported in Refs. 16–21 (these lists of references are by no means exhaustive as the number of publications on Si clusters increases very rapidly).

For Ge, on the basis of mass spectrometry analysis, it has been suggested[5] that stable clusters derive from a basic unit which is a six-atom ring with a flat or puckered configuration, and a ''hat'' can be placed on the bonds extending out of the plane of the ring thus forming more six-atoms rings. These structures, as well as the spherical Si clusters, can be regarded as *ad hoc* version of the fullerene cages. No detailed calculation seems to have been developed for Pb. However, early calculations, based on simple two-body central potentials,[22] indicate that clusters of metallic elements are formed by tetrahedrons and have a nearly spherical form and a high density. This metallic character, however, have also been found in recent tight-binding molecular dynamics calculations of silicon clusters of size $N=60$.[23]

On the basis of these results the calculations were initialized by using (i) an elongated structure formed by a ribbon, or a folded ribbon, of hexagons, (ii) a spherical cage of the fullerene type, and (iii) an unreconstructed bulk fragment. This last one was used to assess the possibility of the formation of structures similar to the ones of the parent crystalline lattice. A detailed investigation of configurations belonging to these three main sets seemed unnecessary. However, the stability of the optimized structure was tested by using the configuration of energy minimum as an input for a further minimization. Furthermore, for each N value, a further short search for clusters of size $N-1$ and $N+1$ was made by starting from the optimum configuration for the size N.

The results of the calculations are summarized in the following figures and tables. The parameters reported in the tables describe the electronic structure and the geometry of the clusters and illustrate the relationships of these quantities to the ones of the crystalline solid. The quantities shown are the binding energy per atom, the ionization potential, the maximum interatomic distance, the average bond length and angle (referred to the central atom in the cluster), and the maximum vibrational frequency (E_b, I_p, $R_{\max}$, R_b, Θ, and $f_{\max}$, respectively). In the tables two values reported under the same heading indicate that fluctuations within the shown limits were regularly found for E_b values differing by ~ 0.02 eV. An omitted datum indicates an insufficiently precise evaluation.

A. Monoelemental clusters

The parameters of monoelemental Si, Ge, and Pb clusters are reported in Tables I, II, and III, respectively.

The smaller clusters ($N \leqslant 10$) illustrate the quality of the minimization. For $N=3,4,6$ in silicon energy minima were found to be the approximate isosceles triangle, the planar rhombus, and the distorted bipyramid. Equivalent structures were found for the minima in Ge and Pb. The values in parentheses in Table I are results of local-density approximation (LDA) and *ab initio* calculations and experimental values. The references for E_b, R_b, Θ, and $f_{\max}$ are the calculations in Refs. 14, 12, 11, and 15. The sources for $f_{\max}$ and I_p are the calculations and experiments reported in Refs. 10 and 15. A good quantitative agreement between these data and AM1 is observed. Worse results are obtained from MNDO. Furthermore, for $N=3,6$, MNDO leads to noticeably different values of Θ for clusters whose E_b values have only slight differences. However, as shown by the values in parentheses, this discrepancy is not uncommon as a similar spread has also been found in Ref. 11.

For all the three elements AM1, MNDO, and PM3 lead-to noticeably different values of E_b, I_p, and $f_{\max}$. Similar divergent results have also been found for the band structure and the characteristic energies of oxygen donors in Ge reported in Ref. 24, where a comparison among PM3, AM1, and MNDO has also been made. However, in our calculations the structural properties of the clusters appear consistently evaluated by the three Hamiltonians. In fact, the evident homogeneity of the geometrical parameters $R_{\max}$, R_b, and Θ for all sizes and types of clusters of the three elements indicates that AM1, MNDO, and PM3 lead, in essence, to the same optimized structure. Furthermore, the evaluation of E_b in Si, especially for large N, appears fairly insensitive to the detailed form of the Hamiltonian, this fact being attributable to the superior parametrization available for this element.

TABLE I. Si clusters. Comparison with other calculations and with experiments. The quantities shown are the binding energy E_b, the ionization potential I_p, the maximum interatomic distance R_{max}, the average bond length R_b, the average bond angle Θ, and the maximum vibrational frequency f_{max}. E_b shows the decrease with respect to the atomic energy. R_b and Θ are refered to the central atom in the cluster. An omitted datum indicates an inaccurate evaluation.

N	E_b (eV)	I_p (eV)	R_{max} (Å)	R_b (Å)	Θ (deg)	f_{max} (cm^{-1})
			Small			
3(MNDO)	3.32	7.0	3.6	2.0	91–110	875.0
6(MNDO)	3.15	5.71–6.62	5.1–6.6	2.7	60–90	807.0
3(AM1)	2.53 (2.45,2.63)	7.9 (7.92)	2.4	2.05 (2.17,2.56)	70 (80,180)	661 (582)
6(AM1)	3.3 (3.26,3.6)	7.9–8.19	4.8	2.39 (2.33,2.65)	90.0	583.0
			Elongated			
14(MNDO)	4.3	7.0	10.5	1.92	121.0	893.0
29(MNDO)	4.1 (3.93)		19.2	2.2	112.0	862.0
36(MNDO)	4.43 (~4.2)	6.1	14.0	2.2	111.0	843.0
48(MNDO)	4.42	6.6	21.0	2.2	120.0	746.0
90(MNDO)	4.45	5.3	17.5	2.27	106.0	
14(AM1)	3.90	8.2	11.1	2.2	125.0	750.0
28(AM1)	4.36	8.0	13.2	2.4	112.0	590.0
48(AM1)	4.43	7.4	17.2	2.4	116.0	523.0
			Spherical cage			
14(MNDO)	4.17	6.3–6.5	7.01	2.61	70–100	791.0
24(MNDO)	4.49	6.3	9.10	2.5–2.6	86.0	781.0
28(MNDO)	4.73 (~4.05)	6.5	8.50	2.44	85.0	781.0
48(MNDO)	5.14 (~4.7)	5.6	11.0	2.45 (~2.275)	102.0	781.0
72(MNDO)	5.10		13.0	2.44	101.0	
14(AM1)	4.23	6.44–7.71	5.0–6.6	2.8	80.0	690.0
28(AM1)	4.43	7.84	8.60	2.55	85.0	690.0
50(AM1)	4.60	7.71	12.5	2.78	103.0	587.0

TABLE II. Ge clusters. Symbols as in Table I.

N	E_b (eV)	I_p (eV)	R_{max} (Å)	R_b (Å)	Θ (deg)	f_{max} (cm^{-1})
			Small			
6(MNDO)	2.26	5.75	4.35	2.56	96.0	373.0
6(AM1)	4.23	8.04	4.53	2.51	85.2	308.0
			Elongated			
14(MNDO)	2.5	6.34	12–14	2.38–3.03	105.0	404.0
28(MNDO)	2.8	6.02	15.6	2.40	112.0	349.0
48(MNDO)	2.9	6.3	17.13	2.38	114.0	377.0
63(MNDO)	2.7	4.95–5.04	17.4–19	2.4	104.0	382.0
89(MNDO)	2.7	4.73	20.0	2.5	106.0	
14(AM1)	5.72	9.71	9.1	2.34	100.0	470.0
28(AM1)	5.65	7.28	14.2	2.30	120.0	409.0
48(AM1)	5.85	6.9	16.2	2.30	122.0	401.0
			Spherical cage			
14(MNDO)	2.73	5.60	7.01	3.30	81.0	331.0–371.0
24(MNDO)	2.80	5.8	8.6	2.80	89.0	371.0
49(MNDO)	3.03	5.9	13.4	2.88	104.0	373.0
72(MDNO)	3.10	5.6	14.0	2.62	104.0	
24(AM1)	5.90	8.0	7.71	2.87	73.0	413.0
30(AM1)	5.96	7.7	8.40	2.50	86.0	413.0
50(AM1)	6.10	8.3	11.0	2.80	100.0	
72(AM1)	6.16	8.3	12.2	2.44	102.0	

TABLE III. Pb clusters. Symbols as in Table I.

N	E_b (eV)	I_p (eV)	R_{max} (Å)	R_b (Å)	Θ (deg)	f_{max} (cm^{-1})
			Small			
6(MNDO)	2.9	7.99	4.3	3.1	80.0	176.0
6(PM3)	1.64	7.04	5.6	3.2	85.0	203.0
			Elongated			
14(MNDO)	3.22	7.47	10.42	2.84	100.0	184.0
28(MNDO)	3.38	7.04	14.2	3.10	95.0	184.0
48(MNDO)	3.34	6.70	20.0	2.89	110.0	184.0
14(PM3)	1.66	7.13	15.25	2.57	116.0	245.0
28(PM3)	1.99	7.10	14.5	2.94	104.0	199.0
48(PM3)	1.80	7.41	20.0	2.80	115.0	
			Spherically joined tetrahedral			
14(MNDO)	3.41	7.29	8.2	3.06–3.12	76.0–95.0	175.0
24(MNDO)	3.37	6.76	9.2	3.00	87.0	167.0
30(MNDO)	3.53	6.62	10.67–11.5	3.52	86.0	167.0
50(MNDO)	4.00	6.50	14.21–15.0	3.17	95.0	
14(MP3)	1.81	7.40	7.11	3.00	81.0	220.0
24(PM3)	2.06	7.14	13.3	3.16	91.0	231.0

For $N \geq 14$ two series of structures, one elongated and one approximately spherical, were found for Si, Ge, and Pb. The calculations initiated with a crystalline fragment invariably evolved into one of these two forms, the final geometry depending on the initial cluster being a cube or an elongated parallelepiped. In Si and Ge (Ge clusters representative for both elements are reported in Fig. 1) the elongated clusters consist of stacked rings of five or six atoms joined at the side. Generally the rings are flat and for the smaller N the cluster has a capped termination. Similar structures formed by the stacking of benzenelike rings, also obtained from MNDO calculations, have been reported in Ref. 25 to describe the reconstruction of the $\langle 111 \rangle$ Si surface. The elongated Si clusters of size $N \geq 20$ presented in Ref. 17 have, in comparison with ours, a more regular form and the sixfold rings always have a puckered configuration. In our calculations the flat form of the manyfold rings and of their junction with the dimers in the cluster cuspid indicates that the angular component of the bonding may be underestimated by the semiempirical Hamiltonians.

The spherical clusters of Si and Ge (Fig. 2) consist of atoms with a threefold coordination and fewer atoms with an irregular but higher coordination. The interbonding between these two types of atoms lead to large, nonstacked, pentagonal, hexagonal, and, as shown by the topmost face of Ge_{49} in Fig. 2, also octagonal rings. Rings of these forms with a zigzag distribution have been observed in faulted Si formed during ion or electron irradiation.[26] However, while the rings observed in implanted Si have a puckered configuration, ours are flat, and this points, once more, to a possible miscalculation of the bonding angles. For the spherical clusters the number of atoms with a higher coordination increases with the increase of N and, as shown by the comparison of Ge_{49} and Ge_{72}, the cluster evolves towards a more packed form. This last character appears also from the sublinear increase of R_{max} with $N^{1/3}$ shown by the data in the tables.

An increase of the average bonding length R_b is generally observed in passing from Si to Ge and Pb and this is obviously consistent with the delocalized s and p bonding of the

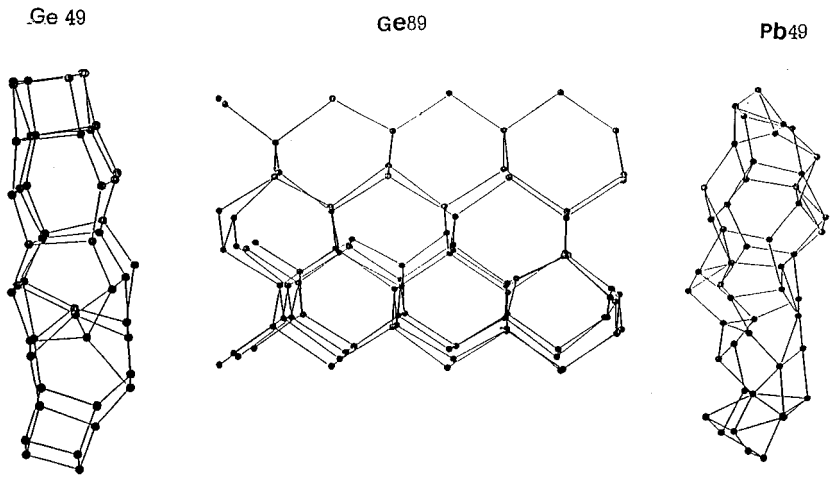

FIG. 1. Elongated clusters. Structure of Ge_{49}, Ge_{89}, and Pb_{49}. MNDO calculations.

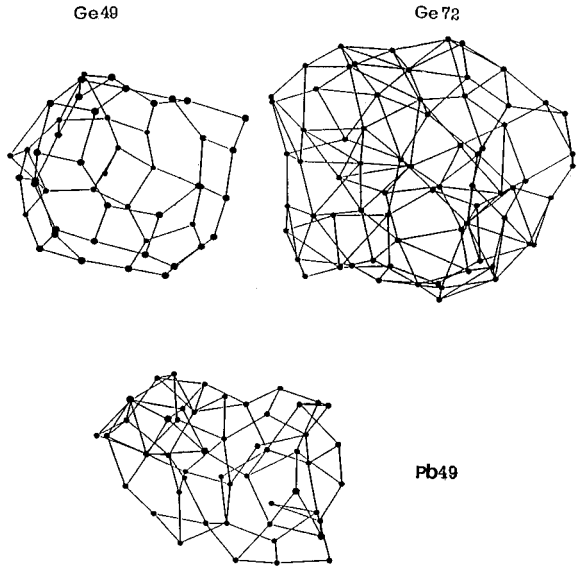

FIG. 2. Spherical clusters. Structure of Ge_{49}, Ge_{72}, and Pb_{50}. MNDO calculations.

metallic element. However, the values of $R_{\max}$ and Θ in Pb are regularly equal to, or smaller than, the ones in Si and Ge and this indicates the formation of structures with a high packing density. This characteristic is clearly illustrated by the comparison between the elongated Ge_{49} and Pb_{49} in Fig. 1 and, to less extent, by the spherical Ge_{49} and Pb_{49} in Fig. 2. It is seen that the high density of Pb results from atoms being brought into the cluster interior so that the cluster structure consists of interlocked pyramids of a somewhat distorted form.

For all the three elements the binding energy of the spherical clusters decreases with the cluster size for large N and that of the elongated clusters remains approximately constant (no attempt has been made to evaluate exactly the threshold size leading to an energy crossover between the two types of clusters). As shown by the figures, the elongated structures grow by the multiplication of self-similar units, so that the superficial tension per unit remains approximately constant, whereas in the spherical clusters the number of atoms with higher coordination increases for increasing N. We consequently interpret the reduction of E_b in the spherical clusters as a contraction of the surface tension. This interpretation agrees with the conclusions presented in Refs. 17 and 18 and our calculations considerably extend, from the point of view of either the cluster size or the element type, the range of this theory. However, it is noted that, while E_b decreases by approximately 0.4 eV for $24 \leqslant N \leqslant 50$ in Si and Pb, this decrease is limited to 0.2–0.3 eV in Ge. It is not clear at the present stage of the research if this is a physical effect or if it arises from some inadequacy of the parametrization.

A further important aspect of our calculations is that for large spherical Si and Ge clusters Θ changes from an approximately metallic, high-density value (i.e., $\sim$70, 80) to a covalent one ($\sim$100) and we interpret this behavior as the crossover from metallic to covalent bonding. A similar conclusion has been presented in Ref. 17 on the basis of the spatial features of the electronic charge distribution.

In Table I for Si $N=28,36,48$ the values of E_b and R_b obtained in Ref. 18 for clusters of similar size are indicated in parentheses. A reasonable agreement is found on the decreasing trend of E_b. Furthermore, in Ref. 23 the R_b value for icosahedral Si, $N=60$, falls in the range 2.44 Å and this value also favorably compares with MNDO calculations for clusters of the same size, while AM1 evidently overestimates this parameter. For Ge and Pb, taking the crystal as a reference (the experimental value of E_b is 2.06 and 3.85 eV for crystalline Pb and Ge, respectively[27]), E_b in Ge is underestimated by MNDO and overestimated by AM1 almost in the same ratio. In Pb E_b is overestimated by MNDO while PM3 results are in agreement with experiments.

For all the three elements I_p has an approximately metallic behavior as it decreases for increasing values of the cluster size and of $R_{\max}$.[28] On the contrary no clear structure dependence was found for $f_{\max}$. It has been shown in Ref. 22 that the frequency distribution of small clusters lacks the ordered structure of the branches of the crystal. For this reason we describe the cluster vibrational spectrum by using only a gross feature, that is, the maximum frequency. However, even this simple parameter represents a critical part of the calculations as changes of $f_{\max}$ around 10–12 % arise from fluctuations of E_b as small as 0.01–0.02 eV. Provided that an error in the range $\sim$10–12 % is assigned to the evaluation of this parameter, $f_{\max}$ appears to be independent of the type and size of the cluster. However, large breathing modes are clearly observed in the elongated clusters of Si of size $N=14$, these modes being possibly favored by the large surface-to-volume ratio of these clusters. It is further added that for all the three elements the size $N=6$ sets the threshold for the formation of low-frequency vibrations arising from cooperative motions of 4–5 atoms. For instance, for Si $N=3$ the minimum frequency was found to be equal to 153 cm^{-1} (a similar value, that is, 206 cm^{-1}, is reported in Ref. 15) and this value was reduced to 50 cm^{-1} for $N=6$.

B. Compound clusters

The parameters of the compound clusters are reported in Tables IV and V. In these calculations the initial configuration for the energy minimization is obtained from the structure of the optimum monoelemental cluster by replacing a given fraction of covalent atoms with Pb. The spatial distribution of Pb has been varied from a compact configuration, with Pb atoms at a nearest-neighbor distance, to a scattered network distributed on the cluster surface or in its interior. In all cases, however, the content of Pb is low (generally, its fractional value is $\leqslant$0.5). The calculations show that under such conditions the bonding mode has a primary dependence on the total Pb content rather than on the fine details of the cluster composition.

For this reason our analysis is limited to the effects of the Pb content and the results are summarized in Table IV. The quantities reported in the table are the number of Pb atoms (fraction of the total), the binding energies E_b and E_{bc}, and the average values of R_b and Θ of the two components of the cluster. E_b represents the effect of the metal on Si and Ge and is evaluated from the decrease of the energy per atom with respect to a ground-state energy $E_0 = NE_{\text{sem}}$, E_{sem} being the binding energy of the semiconductor atom (i.e., Si or Ge). E_{bc} quantifies the cluster stability. The ground-state en-

TABLE IV. Compound Si-Pb and Ge-Pb clusters. The parameters reported in the table are the number of Pb atoms (fraction of the total), the binding energy E_b with respect to one atom of Si or Ge, the binding energy E_{bc} with respect to one covalent plus a metallic atom, and the average values of R_b and Θ for the two components of the cluster. For Si/Pb these averages are taken on bonds Si-Si and Si-Pb for Si and Pb-Pb and Pb-Si for Pb. For Ge/Pb they are taken on Ge-Ge and Ge-Pb for Ge and Pb-Pb and Pb-Ge for Pb. In Tables IV and V, *S* and *E* indicate spherical and elongated clusters, respectively.

N	Pb fraction	E_b (eV)	E_{bc} (eV)	R_b (Å)	Θ (deg)	R_b (Å)	Θ (deg)
				Si		Pb	
			Metallic-covalent bonding				
14 *S*	0.30	10.3	4.0	3.30	70.0	3.50	95.0
14 *S*	0.50	15.1	3.9	2.90	70.0	3.10	105.0
14 *E*	0.28	10.3	3.9	2.50	74.0	2.44	111.0
14 *E*	0.50	14.8	3.7	2.50	85.0	2.90	96.0
24 *S*	0.33	12.0	4.3	3.30	90.0	2.97	89.5
24 *S*	0.50	15.2	4.0	2.51	87.0	3.13	84.5
50 *S*	0.30	11.0	4.6	2.76	82.0	3.40	107.0
50 *S*	0.46	14.5	4.3	2.57	84.2	3.11	110.0
			Covalent bonding				
48 *E*	0.41	13.1	3.78	2.16	113	2.50	126.0
48 *E*	0.50	16.0	3.82	2.32	101	2.60	124.0
72 *S*	0.20	8.5	4.13	2.49	100	2.67	106.0
72 *S*	0.35	11.6	3.86	2.53	101	2.62	101.0
72 *S*	0.41	13.7	4.16	2.86	87	2.63	102.0
				Ge		Pb	
			Metallic-covalent bonding				
14 *E*	0.28	11.7	3.2	2.56	100.0	2.60	104.0
14 *E*	0.50	18.3	3.6	3.29	75.0	2.84	91.0
14 *S*	0.35	14.0	3.3	3.00	89.0	3.50	75.0
14 *S*	0.50	18.0	3.5	3.00	96.0	3.20	98.0
24 *E*	0.48	16.6	3.32	2.85	81.5	2.62	101.0
24 *S*	0.29	12.1	3.5	3.10	90.0	3.50	70.0
24 *S*	0.38	14.7	3.6	3.30	95.0	3.00	81.0
24 *S*	0.54	19.1	3.5	3.60	93.0	2.83	71.0
50 *S*	0.3	11.9	3.2	2.98	85.3	3.41	99.1
50 *S*	0.5	16.7	3.4	3.17	89.0	3.15	99.0
			covalent bonding				
48 *E*	0.31	11.6	3.2	2.62	106.0	2.85	103.0
48 *E*	0.41	15.4	3.3	2.56	102.0	2.75	112.0
63 *E*	0.25	9.9	3.3	2.45	100.0	2.74	111.0
63 *E*	0.41	15.9	3.4	2.45	100.0	2.59	103.0
89 *E*	0.25	10.6	3.3	2.58	101.0	2.44	110.0
89 *E*	0.41	15.7	3.3	2.56	100.0	2.61	108.0

ergy used for this evaluation is $E_0 = N_{\rm sem}E_{\rm sem} + N_{\rm met}E_{\rm met}$, where $N_{\rm sem}$ and $N_{\rm met}$ are the number of semiconductor and metallic atoms in the cluster and $E_{\rm sem}$ and $E_{\rm met}$ are the corresponding atomic energies.

Table V reports the average values of the diagonal terms of the σ and π bond-order matrix components. The corresponding quantities of the monoelemental clusters of the same size are indicated in parentheses.

From Table IV it is evident that the need of adapting the covalent structure with short R_b and large Θ to one with opposite requisites leads to a dilatation of the R_b of the semiconductor atoms and to an increase of Θ of the metallic ones. As shown by the examples in Table V, this results from the parallel increase of the πp components of both Si and Pb though in Pb there is also a large decrease of the σ component. These effects (indicated in Table IV as metallic-covalent bonding) are substantial in the smaller clusters, whereas in the larger ones the bonding has, for both components, a nearly covalent character. We interpret this result as an increase of the spatial spread of the metallic orbitals made possible by the larger size of the cluster. This spread has to be conceived as the metallic analog of the πp bonding chains of the silicon surfaces and it leads to the prevalence of the covalent type of bonding at short range.

The data of Table IV show that the low binding energy of the Pb atom, which in MNDO is 1.29 and 1.39 times smaller than that of Si and Ge, noticeably reduces E_b. The effect, however, has a remarkably sublinear dependence on the Pb

TABLE V. Values per atom of the on-diagonal σ and π components of the bond-order matrix. The values in parentheses are the analogous quantities for the monoelemental clusters of the same size.

N	Element	$s\sigma$	$p\sigma$	$p\pi$
		Silicon cluster with 0.3 Pb content		
14 E	Si	0.35 (0.45)	0.47 (0.40)	0.17 (0.15)
14 E	Pb	0.039 (0.84)	0.842 (0.77)	0.124 (0.15)
50 S	Si	0.41 (0.44)	0.51 (0.45)	0.07 (0.01)
50 S	Pb	0.03 (0.323)	0.86 (0.565)	0.11 (0.11)

content. Furthermore, even if the bonding of the semiconductor atoms to the cluster is greatly increased by the metallic inclusion, E_{bc} is not uniformly lower than the binding energy of the monoelemental clusters. This trend is apparent in Si/Pb and suggests that these clusters might have a lower stability than the silicon ones. It is thought that our data are not systematic enough to clearly infer the dependence of E_b and E_{bc} on the cluster size. In their present form the only legimate conclusion is that E_b and E_{bc} do not decrease the increase of the cluster size. As in compound clusters the metallic inclusion is the primary factor for the lowering of the binding energies, this behavior appears attributable to the spread of the metallic orbitals which takes place in the large clusters and reduces the metallic character of the bonding.

Our concluding comments and caveats are on the quality of the energy minimization. At the present state of the research we are not able to indicate precise and systematic trends on the errors due to the minimization procedure. However, it has been found, as expected, that the quality of the minimization generally decreases for increasing N and this adverse effect is particularly evident for elongated clusters of every composition. To assess in an independent way the stability of these clusters two test calculations were made. In the first one the cluster was modified by the addition of capping H atoms. It was found, in fact, that the positions of boundary atoms had the maximum change during minimization and this suggested that the open termination of the elongated clusters was responsible for the decrease of the quality of the minimization. Calculations using clusters of size $N\sim40$ with a variable content of H did not show any significant alteration of the binding energy. However, the structure of the cluster showed a critical dependence on the H content and cluster fragmentation was observed for an ''excess'' H (no attempt was made at an exact evaluation of this critical H content). In the second series of calculations the DRC paths, following an initial impulse of kinetic energy of value in the thermal range ($\sim$30 meV), were calculated for the elongated silicon clusters of size $N=48$ and 90. The result of this input energy was a displacement $\sim$0.08 Å averaged over a transient of a duration 40 fs. These values approximately coincide with the thermal elongation of the atoms in the silicon crystal as obtained from our molecular dynamics calculations. These two calculations supports the conclusion that the larger clusters are, at least on average, closed-shell structures and H passivators are not needed. Furthermore, their structure has kinematic stability though this can be proved only for the short time of the DRC calculations.

IV. CONCLUSIONS

We have studied the properties of monoelemental Si, Ge, and Pb clusters and of compound Si-Pb and Ge-Pb clusters of size $10\leqslant N\leqslant90$ by using semiempirical methods of the MO type.

The calculations indicate that for the monoelemental clusters of all three elements elongated and spherical structures are both possible, the latter lying lower in binding energy at large N. The structure of Ge and Pb has only a weak similarity with the ones presented elsewhere,[5,22] as bond relaxation significantly alters the cluster structure with respect to either the cage formed by sixfold rings presented in Ref. 5 or the interlocked tetrahedra presented in Ref. 22.

Remarkable size-dependent effects have been found in compound clusters. These clusters show, in fact, either a bonding intermediate between metallic and covalent or a somewhat distorted covalent bonding and the propensity to the one or the other form depends on the size of the cluster.

Finally, we reiterate that semiempirical methods allow the study of clusters of noticeably larger size than the ones studied by *ab initio* methods. However, problematic aspects in the parametrization and minimization procedure must also be accounted for.

ACKNOWLEDGMENTS

Many thanks are due to Dr. J. P. Stewart for his help with the use of MOPAC.

[1] L. Li, C. Koziol, K. Wurm, Y. Hong, E. Bauer, and L. S. Tsong, Phys. Rev. B **50**, 10 834 (1994).
[2] R. G. Zhao, Y. Zhang, and W. S. Yang, Phys. Rev. B **48**, 8462 (1993).
[3] F. Ancilotto, A. Selloni, and R. Car, Phys. Rev. Lett. **71**, 3685 (1994).
[4] F. Ancilotto, A. Selloni, and R. Car, Phys. Rev. B **50**, 15 158 (1994).
[5] T. P. Martin and H. Schaber, J. Chem. Phys. **83**, 2 (1985).
[6] S. N. Khanna and P. Jena, Phys. Rev. Lett. **69**, 1664 (1992).
[7] J. P. Stewart, J. Comput. Chem. **10**, 209 (1989).
[8] A. M. Mazzone, Philos. Mag. Lett. **70**, 93 (1994).
[9] B. W. Dodson, Phys. Rev. B **33**, 7361 (1994).
[10] K. Raghavachari and V. Lagovinsky, Phys. Rev. Lett. **55**, 26 (1985).
[11] P. Ballone, W. Andreani, R. Car, and M. Parrinello, Phys. Rev. Lett. **60**, 271 (1988).
[12] N. Binggeli, J. L. Martin, and J. R. Chelikowsky, Phys. Rev. Lett. **68**, 2956 (1992).
[13] H. Balamane, T. Halicioglu, and W. A. Tiller, Phys. Rev. B **46**, 2250 (1992).
[14] J. C. Grossmann and L. Mitas, Phys. Rev. Lett. **74**, 1323 (1995).
[15] M. Menon and K. R. Subbaswamy, Phys. Rev. B **47**, 12 754 (1993).

[16] J. R. Chelikowsky and J. C. Phillips, Phys. Rev. Lett. **63**, 1653 (1989).
[17] E. Kaxiras and K. Jackson, Phys. Rev. Lett. **71**, 727 (1993).
[18] E. Kaxiras, Phys. Rev. Lett. **64**, 551 (1990).
[19] J. Pan and M. V. Ramakrishna, Phys. Rev. B **50**, 15 431 (1994).
[20] J. Pan and M. V. Ramakrishna, Phys. Rev. B **50**, 15 431 (1994).
[21] U. Rothlisberger, W. Andreoni, and M. Parrinello, Phys. Rev. Lett. **72**, 665 (1994).
[22] M. R. Hoare and P. Pal, J. Cryst. Growth **17**, 77 (1972).
[23] M. Menon and K. R. Subbaswamy, Chem. Phys. Lett. **219**, 219 (1994).
[24] P. Deak, B. Schroder, A. Annen, and A. Scholz, Phys. Rev. B **48**, 1924 (1993).
[25] Y. G. Hao and L. Roth, in *Computer-Based Microscopic Description of the Structure and Properties of Materials*, edited by J. Broughton, W. Krekow and S. T. Pontelides, MRS Symposia Proceedings Vol. 63 (Materials Research Society, Pittsburgh, 1986), p. 167.
[26] A. Parisini and A. Bourret, Philos. Mag. A **67**, 605 (1993).
[27] M. J. Baskes, Phys. Rev. B **46**, 2727 (1992).
[28] M. Seidl and J. P. Perdew, Phys. Rev. B **50**, 8 (1994).